J Dent Res 77(4): 589-602, April, 1998

Mechanical Characterization of Dental Ceramics by Hertzian Contacts

I.M. Peterson[1]*, A. Pajares[1], B.R. Lawn[1], V.P. Thompson[2], and E.D. Rekow[2]

[1]Materials Science and Engineering Laboratory, National Institute of Standards and Technology, Gaithersburg, Maryland 20899; and [2]Dental School, Orthodontics, University of Medicine and Dentistry of New Jersey, Newark, New Jersey 07103; *to whom correspondence should be addressed

Abstract. Hertzian indentation testing is proposed as a protocol for evaluating the role of microstructure in the mechanical response of dental ceramics. A major advantage of Hertzian indentation over more traditional fracture-testing methodologies is that it emulates the loading conditions experienced by dental restorations: Clinical variables (masticatory force and cuspal curvature) identify closely with Hertzian variables (contact load and sphere radius). In this paper, Hertzian responses on four generic dental ceramics systems—micaceous glass-ceramics, glass-infiltrated alumina, feldspathic porcelain, and transformable zirconia—are presented as case studies. Ceramographic sectioning by means of a "bonded-interface" technique provides new information on the contact damage modes. Two distinct modes are observed: "brittle" mode, classic macroscopic fracture outside the contact (ring, or cone cracks), driven by tensile stresses; and "quasi-plastic" mode, a relatively new kind of deformation below the contact (diffuse microdamage), driven by shear stresses. A progressive transition from the first to the second mode with increasing microstructural heterogeneity is observed. The degree of quasi-plasticity is readily apparent as deviations from ideal linear elastic responses on indentation stress–strain curves. Plots of threshold loads for the initiation of both fracture and deformation modes as a function of indenter radius constitute "damage maps" for the evaluation of prospective restoration damage under typical masticatory conditions. The degree of damage in both modes evolves progressively with load above the thresholds. Strength tests on indented specimens quantify sustainable stress levels on restoration materials after damage. The most brittle responses are observed in the fine glass-ceramics and porcelain; conversely, the most quasi-plastic responses are observed in the coarse glass-ceramics and zirconia; the medium glass-ceramics and alumina exhibit intermediate responses. Implications of the results in relation to future materials characterization, selection, and design are considered in the clinical context.

Key words: ceramics, Hertzian contact, quasi-plasticity, strength.

Received December 31, 1996; Last Revision August 11, 1997; Accepted August 28, 1997

Introduction

Ceramics are promising materials for dental restorations because of their high wear resistance, chemical inertness, and, above all, aesthetics. Specific ceramic types in use or under consideration include modifications of conventional feldspathic porcelains, glass-ceramics, glass-infiltrated aluminas, and transformation-toughened zirconias (Giordano, 1996). Among the relevant mechanical properties are strength and lifetime under typical oral conditions, and machinability for intra-oral adjustments and CAD/CAM operations (Rekow, 1992, 1993). Ceramic restorations are subject to premature clinical failure under repetitive occlusal contact. Porcelain and glass-ceramic molar full-crown restorations, for example, exhibit clinical failure rates of 2 to 4% after two years of function, rising to 20 to 25% after 4 to 5 years (Hankinson and Cappetta, 1994; Kelsey *et al.*, 1995). Such failures are consistent with experience from fatigue testing on ceramics (Ritchie, 1988; Lathabai and Lawn, 1989; Lathabai *et al.*, 1989, 1991; Dauskardt *et al.*, 1990; Suresh, 1991; Dauskardt, 1993). Conservatively, restorations have to withstand masticatory forces of 200 N and more than 10^7 cycles (DeLong and Douglas, 1983; Anusavice, 1989; Phillips, 1991; Craig, 1997) at contacts between opposing cusps of characteristic radii of 2 to 4 mm (Wheeler, 1958). Thus far, attempts to gain insight into such failures have been limited to routine strength- and toughness-testing protocols (Kappert and Knode, 1993; Seghi and Sorensen, 1995; Giordano, 1996), and to post-failure examinations of laboratory and clinical specimens (fractography) (Kelly *et al.*, 1990, 1995; Thompson *et al.*, 1994; Harvey and Kelly, 1996). Fundamental studies of interrelations between the material microstructure and the underlying failure mechanisms, especially in relation to occlusal contact conditions, are conspicuously lacking.

A methodology using contacts with spherical indenters has been developed in our laboratories to characterize mechanical properties of brittle materials. It is based on the Hertzian fracture test used in ideally brittle solids (Hertz, 1896; Roesler, 1956; Frank and Lawn, 1967; Langitan and Lawn, 1970; Wilshaw, 1971; Lawn and Wilshaw, 1975), but has been modified to identify and evaluate new kinds of

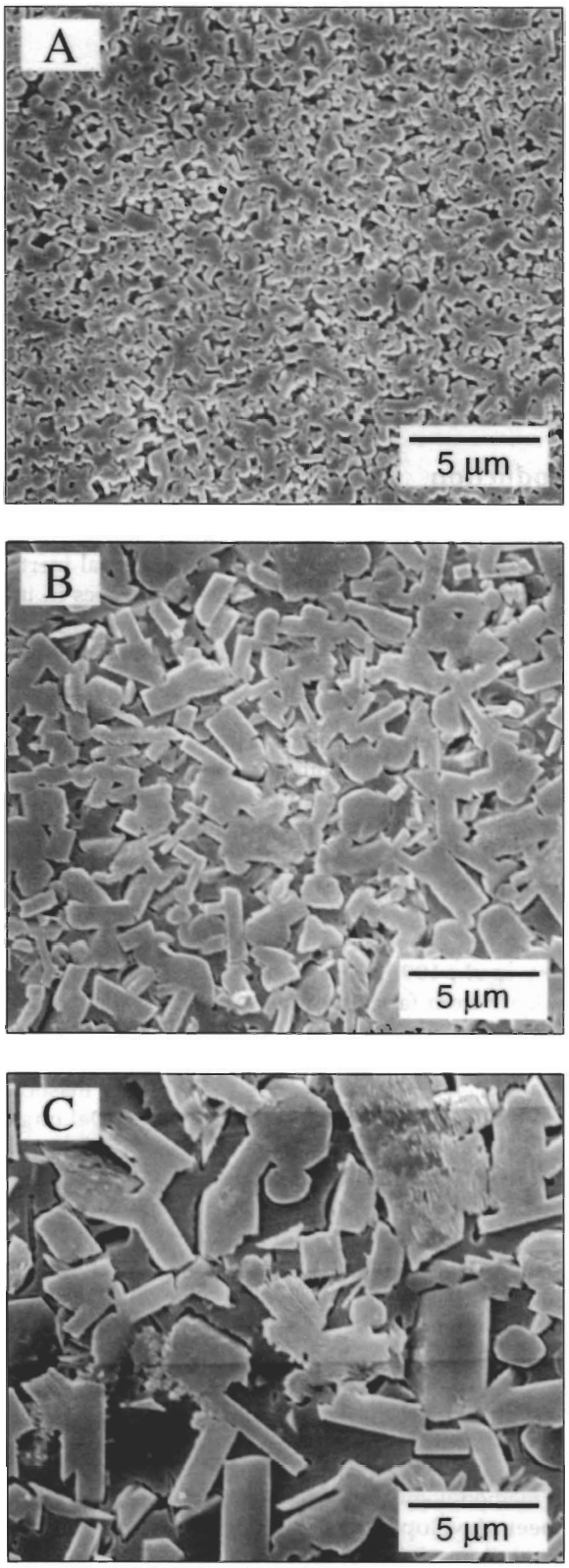

Figure 1. Scanning electron micrographs showing microstructures of micaceous MGC glass-ceramics (Corning): (A) "fine", F-MGC; (B) "medium", M-MGC; (C) "coarse", C-MGC. Surfaces etched with 10 wt% ammonium bifluoride in water for 20 s to reveal mica platelets in glass matrix and gold-coated. Secondary electron images.

damage accumulation in the latest generation of toughened ceramics (Guiberteau *et al.*, 1993, 1994; Cai *et al.*, 1994b; Lawn *et al.*, 1994a; Padture and Lawn, 1994). Whereas in ideally brittle materials, contact failure occurs by the growth of a single macroscopic tensile cone crack ("brittle" mode), in tougher ceramics, failure occurs by evolution of a diffuse subsurface zone of microscopic shear cracks or faults ("quasi-plastic" mode) (Lawn *et al.*, 1994a). The quasi-plasticity is macroscopically analogous to the yield zones that occur beneath contacts in metals (Tabor, 1951); microscopically, however, the shear fault mechanism (Lawn *et al.*, 1994a) differs fundamentally from the dislocation motion that characterizes flow in metallic structures. The Hertzian test has been especially valuable in demonstrating the critical role of microstructure in these two entirely different damage modes. Experimentally, the test is the essence of simplicity, requiring only a hard ball bearing for an indenter. Yet it is uniquely powerful in the insights it provides into the damage modes. The test also lends itself to extension to fatigue testing, *via* repeated normal contact (Guiberteau *et al.*, 1993; Cai *et al.*, 1994a; Padture and Lawn, 1995a; Pajares *et al.*, 1995b; White *et al.*, 1995). Moreover, because it samples damage in the short-crack region, it bears closely on microstructure-sensitive properties like strength and wear resistance. Most important, the test simulates oral loading conditions much more compellingly than conventional mechanical tests, and is characterized by variables that have direct clinical relevance, notably contact (occlusal) load and indenter (cuspal) radius. The first applications of Hertzian contact testing for materials evaluation are beginning to appear in the dental literature (Denry and Rosenstiel, 1995; White *et al.*, 1995).

The goal of this paper is to present data on the role of microstructure on Hertzian contact damage responses of selected generic ceramic systems for dental applications: micaceous glass-ceramics, glass-infiltrated alumina, feldspathic porcelain, and transformable zirconia. We shall devote special attention to the glass-ceramics, because they have been made available to us with a range of well-controlled microstructures. The alumina, porcelain, and zirconia are included for comparison purposes. We shall demonstrate that all these ceramics can be subject to very different modes of damage—classic macroscopic fracture on the one hand, and distributed microdamage on the other. Which damage mode dominates is wholly dependent on the material microstructure; in some instances, a progressive transition from one mode to the other can be induced by appropriate microstructural modifications, *e.g.*, by simple heat treatment. The degree of damage in both modes evolves progressively with load above some microstructure-specific threshold. We indicate how to identify the nature of damage in the contact subsurface zone, and subsequently how to quantify this damage on stress–strain curves and by post-contact strength evaluation. The implications of the test results in relation to clinical conditions will be considered.

In this study, we will demonstrate the usefulness of Hertzian testing as means of mechanical characterization of prospective dental ceramics. It is not our intent to rank or endorse the materials used in this study, nor to present a complete set of data for these materials. Rather, our aim is to

provide the dental researcher with a physical appreciation of the underlying damage processes, and to relate these processes to microstructure.

Materials characterization and Hertzian testing

Materials selection and preparation

In this study, we choose ceramic systems currently under consideration for dental restorations. These systems constitute a spectrum of generic dental ceramics with a broad range of well-characterized microstructures. The microstructures of the chosen materials are shown in Figs. 1 and 2, as follows:

(i) Micaceous glass-ceramics. The micaceous glass-ceramics (MGC) studied here are based on a K_2O–MgF_2–MgO–SiO_2 composition (Corning Inc., Corning, NY) (Chyung *et al.*, 1972, 1974; Grossman, 1991), of the kind used to produce machinable Dicor (Dentsply/Caulk, Milford, DE) for inlays, onlays, and crowns. MGC materials with approximately constant mica platelet volume fraction ≈ 0.60 but with three different platelet dimensions were prepared by controlled crystallization heat treatments for 4 hrs at three different temperatures (Chyung *et al.*, 1972; Fischer-Cripps and Lawn, 1996a). The scanning electron micrographs in Fig. 1 show the "blocky" mica platelets embedded in a glass matrix: at 1000°C, a "fine" (F-MGC) microstructure with platelet thickness ≈ 0.3 μm and diameter ≈1.0 μm (Fig. 1A); at 1060°C, a "medium" (M-MGC) microstructure with platelet thickness ≈ 0.7 μm and diameter ≈ 3 μm (Fig. 1B); at 1120°C, a "coarse"(C-MGC) microstructure with platelet thickness ≈ 1.2 μm and diameter ≈ 8 μm (Fig. 1C). For reference, the microstructure of commercial Dicor MGC (dark) is most closely represented by the F-MGC material. The porosities in each case were < 1 vol%.

(ii) Glass-infiltrated alumina. Another material type used in this study is a commercial dry-pressed, sintered alumina infiltrated with lanthanum–aluminosilicate glass, designed for use in the Celay system (Vita Zahnfabrik, Bad Sackingen, Germany) (Kappert and Knode, 1993; Seghi and Sorensen, 1995; Giordano, 1996). Partially sintered alumina preform blanks of ≈30% porosity and pore size from 1 to 5 μm (Vita Celay InCeram) were machined into bars 3 x 4 x 25 mm and infiltrated with glass (Vita In-Ceram A3.5) for 6 hrs at 1170°C. After the blanks were cooled, the excess glass was ground away with a 10-μm diamond wheel. A scanning electron micrograph of the material after infiltration (Fig. 2A) reveals the alumina superstructure (dark phase) and infiltrated glass (light phase).

(iii) Feldspathic porcelain. Porcelain is widely used as a veneer for metal–ceramic restorations. This material serves as a benchmark material for comparison. The specific material used in this study was a modified feldspathic porcelain Vita Mark II (Vita Zahnfabrik, Bad Sackingen, Germany) intended for machined inlay restorations in the CEREC system (Siemens, Bensheim, Germany). A scanning electron micrograph of a polished and lightly etched specimen surface is shown in Fig. 2B. The microstructure consists of a glass matrix containing particles measuring between 1 and 7 μm, some of which are crystalline- phase sanidine.

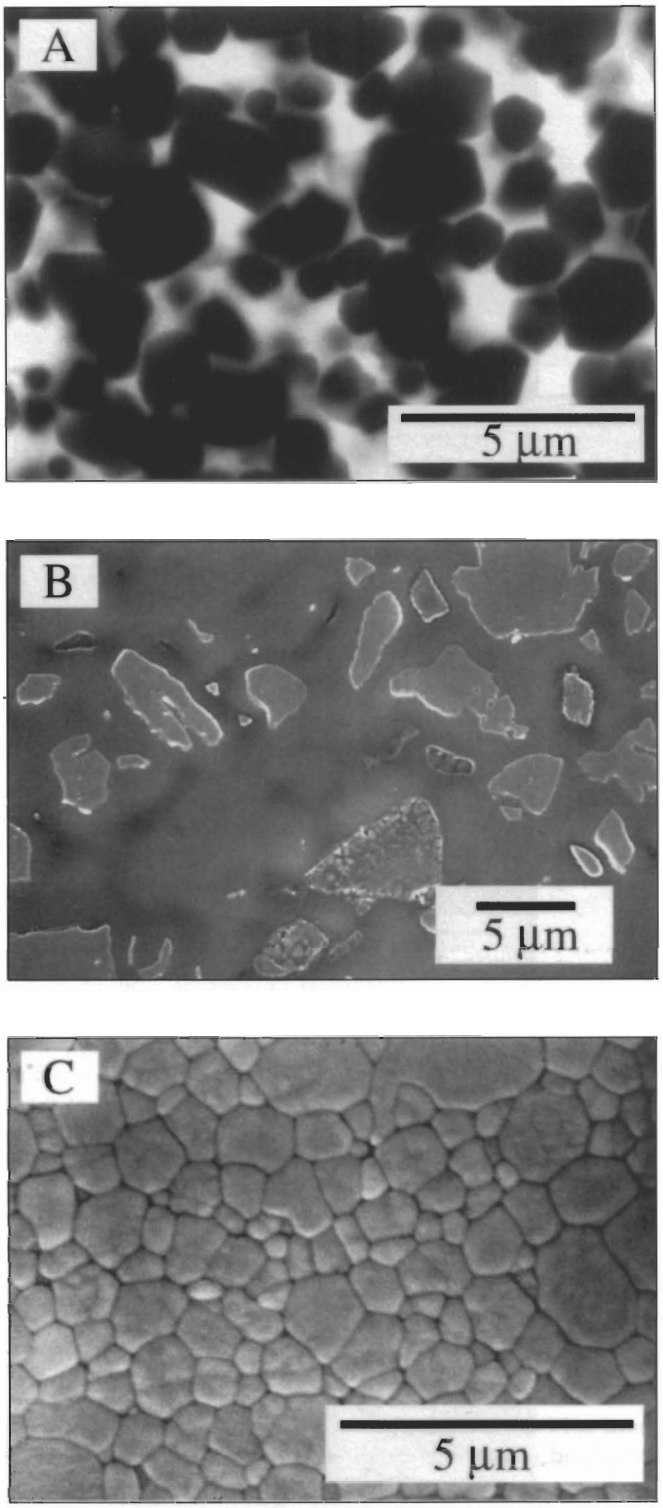

Figure 2. Scanning electron micrographs showing microstructures of selected ceramics. (A) Infiltrated alumina ceramic (Vita InCeram for Celay), back-scattered electron image. (B) Feldspathic porcelain (Vita Mark II), surface etched with 10 wt% ammonium bifluoride in water for 60 s, secondary electron image. (C) Yttria tetragonal zirconia polycrystal (Coors Y-TZP), surface thermally etched at 1400°C for 0.5 hr, secondary electron image. Surfaces gold-coated.

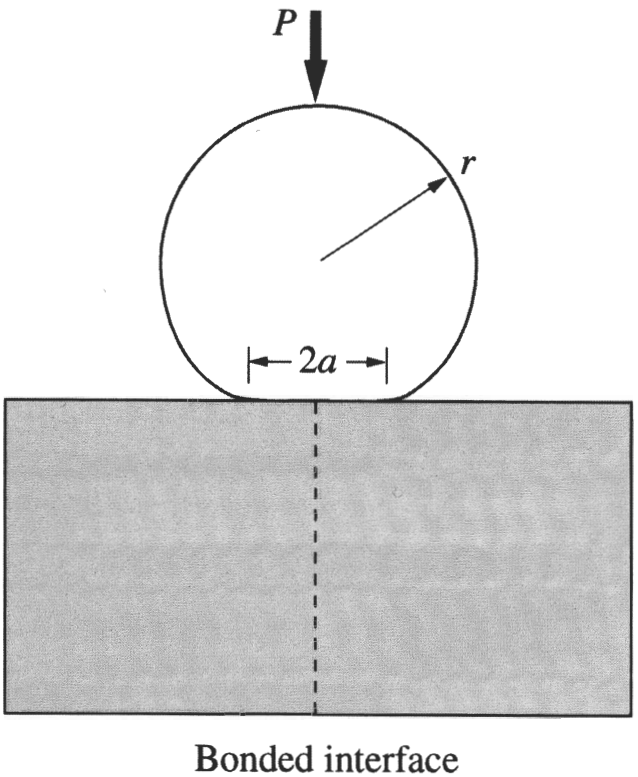

Figure 3. Schematic of Hertzian contact test, with sphere of radius *r* at load *P* over contact radius *a*.

(iv) Yttria-stabilized tetragonal zirconia polycrystal. Yttria-stabilized tetragonal zirconia polycrystal (Y-TZP) is coming under consideration as an alternative high-toughness core material in dental restorations (Giordano, 1996). The zirconia composition used in this study (Coors Ceramics Co., Golden, CO) contains 5.4 wt% yttria stabilizing additive, and has a grain size of about 1 μm. This material exhibits stress-induced transformation toughening. A scanning electron micrograph (Fig. 2C) indicates an equi-axed polycrystalline microstructure.

Bar specimens 3 x 4 x 25 mm were cut from blocks of all materials and polished down to 0.5-μm diamond paste for contact testing and subsequent damage evaluation.

Hertzian contact testing

A schematic of the Hertzian contact test is shown in Fig. 3. A hard sphere of radius *r* is mounted on the underside of the crosshead on a mechanical loading machine. For single-cycle loading, a screw-driven machine is sufficient (Guiberteau *et al.*, 1993; Cai *et al.*, 1994b); for extension to cyclic loading, a hydraulic machine is preferred, so that a sufficiently large number of contacts can be made within a respectably short time interval (Cai *et al.*, 1994a; Padture and Lawn, 1995a). The crosshead is lowered until the sphere is brought into contact with the specimen, and the load is then monotonically increased to a peak value *P*. In the single-cycle tests to be described below, we used tungsten carbide (WC) spheres over a radius range r = 1.98 to 12.7 mm, most commonly at r = 3.18 mm, up to loads of P = 5000 N. High-modulus tungsten carbide spheres are preferred (relative to a softer material closer in modulus to enamel) to ensure a "worst-case" damage configuration and to avoid deformation of the indenters as a result of repeated testing. All tests for this study were performed in single-cycle loading on a universal testing machine (Instron 1122, Canton, MA) in air, at a fixed load–unload crosshead speed 0.2 $mm.min^{-1}$, so as to produce a contact in a manageable time interval ≈ 15 s.

A primary objective of the test methodology is the qualitative identification of underlying damage modes in the candidate ceramic materials. To investigate these modes in both the surface and subsurface regions of the contacts, we used a bonded-interface specimen configuration (Mulhearn, 1959; Guiberteau *et al.*, 1994; Lawn *et al.*, 1994a). Specimens are prepared by the polishing of opposing surfaces of two half-blocks down to 0.5 μm diamond-paste finish. These opposing surfaces are bonded together under small clamping pressure in a machinist hand vise by means of a cyanoacrylate-based adhesive (Loctite Corp., Newington, CT). Top and bottom specimen surfaces perpendicular to the bonded interface are then ground flat with a 10-μm diamond wheel, and the top surface subsequently polished with 0.5-μm diamond paste. To avoid artifacts associated with a soft interlayer, specimens with bonded interfaces wider than 5 μm are rejected (*cf.* typical contact diameter ≈ 200 μm), and the clamping pressure is re-applied during the ensuing contact experiments. (This clamping pressure is negligible compared with the contact stresses.) Here, the bonded-interface specimen was aligned relative to the loading axis, as follows: (i) The specimen was positioned into fixed locating guides on a two-axis traversing micrometer stage on the contact testing machine; (ii) two dummy indentations were made at opposite corners of the specimen surface, and the positions of the specimen at these two locations were recorded by the micrometer; (iii) the specimen was removed from the micrometer stage to the stage of an optical microscope with a video graticule, and the distance of the bonded interface from the centers of the dummy indentations was measured; and (iv) the specimen was replaced on the micrometer stage, and the bonded interface is positioned to intersect the contact load axis. A row of Hertzian indentations was then made on the top surface symmetrically across the bonded interface, at ≈ 3-mm intervals, with a WC sphere of radius r = 3.18 mm. The adhesive was dissolved in acetone, allowing the bonded halves to separate. After the specimen was gold-coated, both the top surface and the interface section surface at the contact sites were examined in a reflection optical microscope with Nomarski interference contrast. Nomarski contrast is extremely sensitive to submicrometer surface offsets down to nanometer scale, and was thereby able to reveal fine detail of the fracture and deformation damage. In this capacity to detect small offsets, Nomarski contrast is generally more sensitive than higher-resolution microscopy, *e.g.*, scanning electron microscopy.

Hertzian tests on polished surfaces (0.5-μm finish) also facilitate quantitative analysis of the damage modes, as follows:

(i) Indentation stress-strain curves. The contact radius, *a*, can be measured from the residual imprint after indentation on gold-coated specimens (Guiberteau *et al.*, 1993). The contact radius was used to calculate an "indentation stress", $p_0 = P/\pi a^2$, and

"indentation strain", a/r (Tabor, 1951; Swain and Lawn, 1969; Swain and Hagan, 1976; Guiberteau *et al.*, 1993; Cai *et al.*, 1994b), enabling indentation stress–strain curves to be constructed. In the present tests, a full range of sphere sizes, r = 1.98 to 12.7 mm, was used to determine these curves. The stress–strain relation for ideal Hertzian elastic contacts is a straight line through the origin, with slope governed by the Young's modulus E of the specimen material,

$$p_0 = (3E/4\pi k)a/r \qquad (1)$$

where $k = (9/16)[(1 - \nu^2) + (1 - \nu'^2)E/E']$ is a dimensionless constant, with ν Poisson's ratio and the prime notation denoting the indenter material (WC) (Timoshenko and Goodier, 1951). Departures from a purely elastic response are consequently measured as deviations from linearity above some critical "yield" stress, quantifying the "quasi-plasticity" component of deformation.

(ii) Load–radius dependence of contact damage. Critical indentation loads for onset of yield, P_Y, and cracking, P_C, were measured as a function of sphere radius, r, for each of the selected materials. In brittle ceramics, P_C was determined by means of an acoustic sensor attached to the specimen surface during indentation (Padture and Lawn, 1995a). Means and standard deviations for P_C were evaluated from 6 indentations at each sphere radius. For less-brittle ceramics that do not produce clear acoustic signals during crack initiation, values of P_C were determined visually from post-failure Nomarski microscopy of specimen surfaces indented at a series of loads in the vicinity of the threshold, with a minimum of 6 indentations at each prescribed load. Uncertainty limits were assessed from the range between the maximum load at which the indentations remained 100% uncracked (lower limit) and the minimum load at which the indentations became 100% cracked (upper limit). The values of P_Y were similarly determined from post-contact inspections of the contact sites, as the loads corresponding to first detectable surface impressions (Davies, 1949).

(iii) Strength degradation tests. The effect of contact damage on subsequent strength is measured by breaking indented specimens in a four-point flexure fixture, with the indentation centered on the tensile side (Marshall *et al.*, 1979). Failure strengths, σ_F, were evaluated from the breaking loads. Means and standard deviations for the strength values were obtained from 3 to 5 breaks for contact loads up to P = 3000 N, with a sphere of radius r = 3.18 mm. To minimize chemical effects in the strength test itself, we placed a drop of silicone oil onto the indentation sites and performed the tests in "fast" fracture ["inert strengths", fracture time < 40 ms (Marshall and Lawn, 1980)]. We examined broken specimens to determine failure origins: *i.e.*, from indentation sites, either ring cracks or subsurface damage zones; or from pre-existing microstructural or surface flaws.

For comparison purposes, we also ran additional strength degradation tests on specimen surfaces after sandblasting with 50-μm silica particles under gas pressure 0.5 MPa with a nozzle–specimen distance 10 mm, to simulate clinical dental preparation protocols. Means and standard deviation strengths were obtained from 4 breaks *per* material.

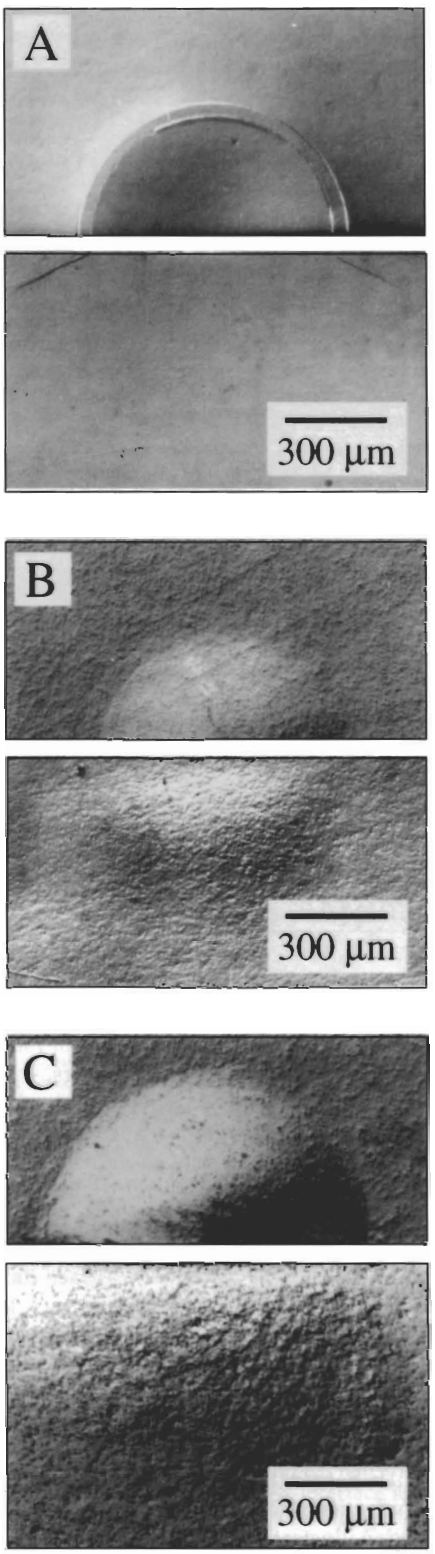

Figure 4. Nomarski optical micrographs, half-surface (upper) and section (lower) views, from bonded-interface specimens of micaceous glass-ceramics, after indentation with a WC sphere, r = 3.18 mm, P = 1000 N: (A) F-MGC, (B) M-MGC, (C) C-MGC.

ANOVA was used to determine the significance of strength changes under the different testing conditions.

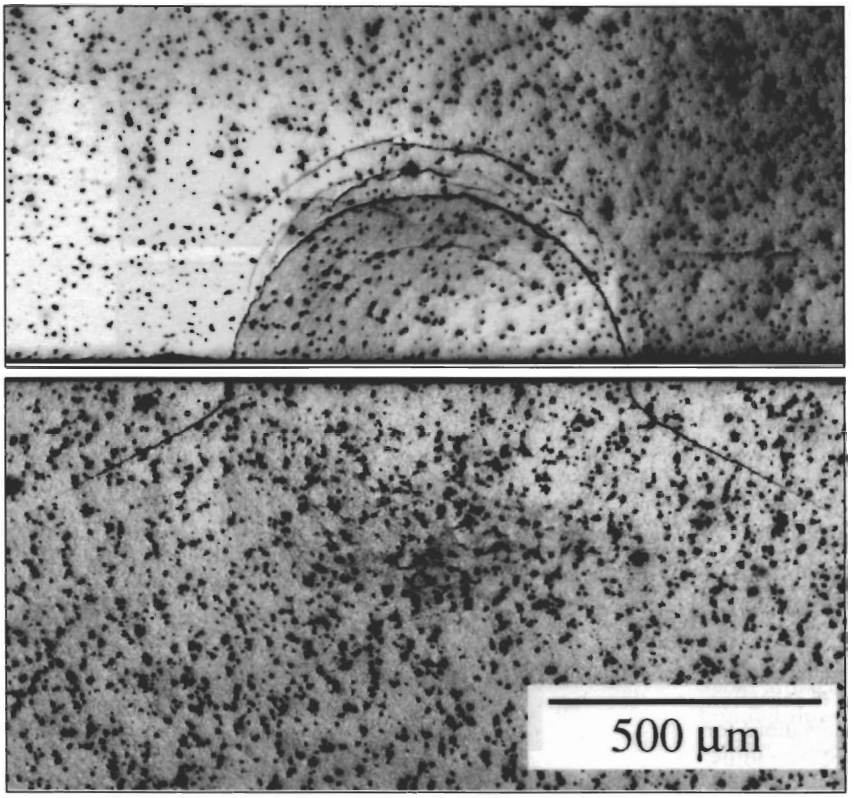

Figure 5. Nomarski optical micrographs, half-surface (upper) and section (lower) views, from bonded-interface specimens of glass-infiltrated alumina, after indentation with a WC sphere, r = 3.18 mm, P = 2500 N. Note some residual porosity in the infiltrated product.

Results

Contact damage patterns from bonded-interface specimens of the selected materials, using WC spheres of radius r = 3.18 mm, are shown in the micrographs in Figs. 4 to 7. Fig. 4 represents the micaceous glass-ceramics, at a contact load P = 1000 N. In F-MGC (Fig. 4A), a near-ideal ring crack pattern is observed. There is a small contact depression within the ring crack in the surface view, indicating the co-existence of quasi-plasticity. In M-MGC (Fig. 4B), ring cracking is very shallow. The surface depression within the surface ring is now deeper, and a corresponding subsurface damage zone is apparent. In C-MGC (Fig. 4C), no ring crack is seen, but quasi-plasticity in both surface and subsurface views is even more apparent.

Fig. 5 shows contact damage in glass-infiltrated alumina, at a load P = 2500 N sufficiently high to produce detectable damage. The pattern reveals a well-developed cone crack together with a faintly visible quasi-plastic surface depression and subsurface yield zone.

Figs. 6 and 7 illustrate how the damage patterns evolve in feldspathic porcelain and yttria-stabilized zirconia with increasing contact load. For the porcelain, the response is primarily brittle, with no visible subsurface yield damage, and with the following crack evolution: at P = 250 N (Fig. 6A), a newly formed ring crack; at P = 750 N (Fig. 6B), extension of the ring crack below the surface; and at P = 1500 N (Fig. 6C), continued evolution of the surface ring into the classic, well-developed cone configuration (Roesler, 1956; Frank and Lawn, 1967). For the zirconia, the response is primarily quasi-plastic, through P = 1000 N (Fig. 7A) and 3000 N (Fig. 7B), with only very shallow ring cracks at 4750 N (Fig. 7C).

Indentation stress–strain data are plotted in Fig. 8. The solid curves in these plots are empirical fits to the data; the dashed lines are asymptotic fits of Eq. 1 to the data in the small stress–strain region. In the MGC series (Fig. 8A), departures from linearity become more pronounced through the sequence F→M→C (Fischer-Cripps and Lawn, 1996a). In C-MGC, enhanced yielding limits the indentation stress to < 3 GPa for indentation strains as high as 0.40. In the alumina (Fig. 8B), extremes in behavior were observed: Infiltration increases the sustainable contact stress at any given contact strain by a factor in excess of 3. Note, however, that the data for the infiltrated alumina still deviate from linearity at higher stresses. In the feldspathic porcelain (Fig. 8C), the data barely deviate from the predicted ideal linear elastic bound. In the zirconia (Fig. 8D), some nonlinearity is apparent at higher stresses (*cf.* infiltrated alumina in Fig. 8B).

Critical load data $P_Y(r)$ for yield and $P_C(r)$ for fracture are plotted in Fig. 9. The solid curves are empirical data fits. The dashed curves through the $P_C(r)$ data for M-MGC in Fig. 9A and zirconia in Fig. 9D indicate formation of only very shallow surface ring cracks (Figs. 4B and 7). There are some omissions: Fig. 9A for C-MGC includes no $P_C(r)$ curve, consistent with the absence of detectable ring cracking (Fig. 4C); Fig. 9C for porcelain includes no $P_Y(r)$ curve, consistent with the absence of detectable yield (Fig. 6). In all of the materials except the porcelain, the critical loads satisfy the condition $P_Y < P_C$ over the data range of contact radius r. The oral zone (shaded) represents a "typical" masticatory force (DeLong and Douglas, 1983; Anusavice, 1989; Phillips, 1991; Craig, 1997) and range of cuspal radius (Wheeler, 1958) for posterior teeth.

Strengths of the micaceous glass-ceramics and infiltrated alumina after contact damage are plotted as a function of indentation load in Figs. 10 and 11, for WC spheres of radius r = 3.18 mm. For reference, values of P_C and P_Y at r = 3.18 mm (from Fig. 9) are indicated in the Figs. as vertical dashed lines. The open boxes at the left axes of the plots are standard deviation bounds of strength values for as-polished unindented specimens, the shaded boxes values for sandblasted specimens. For the indented specimens, the data points with error bars represent means and standard deviations at the specified loads: Open circles represent failures from remote origins (*i.e.*, not intersecting the indentations); closed circles represent failures from the actual indentation sites. Examples of failures from indentation sites are included in the inset micrographs. In the glass-ceramics

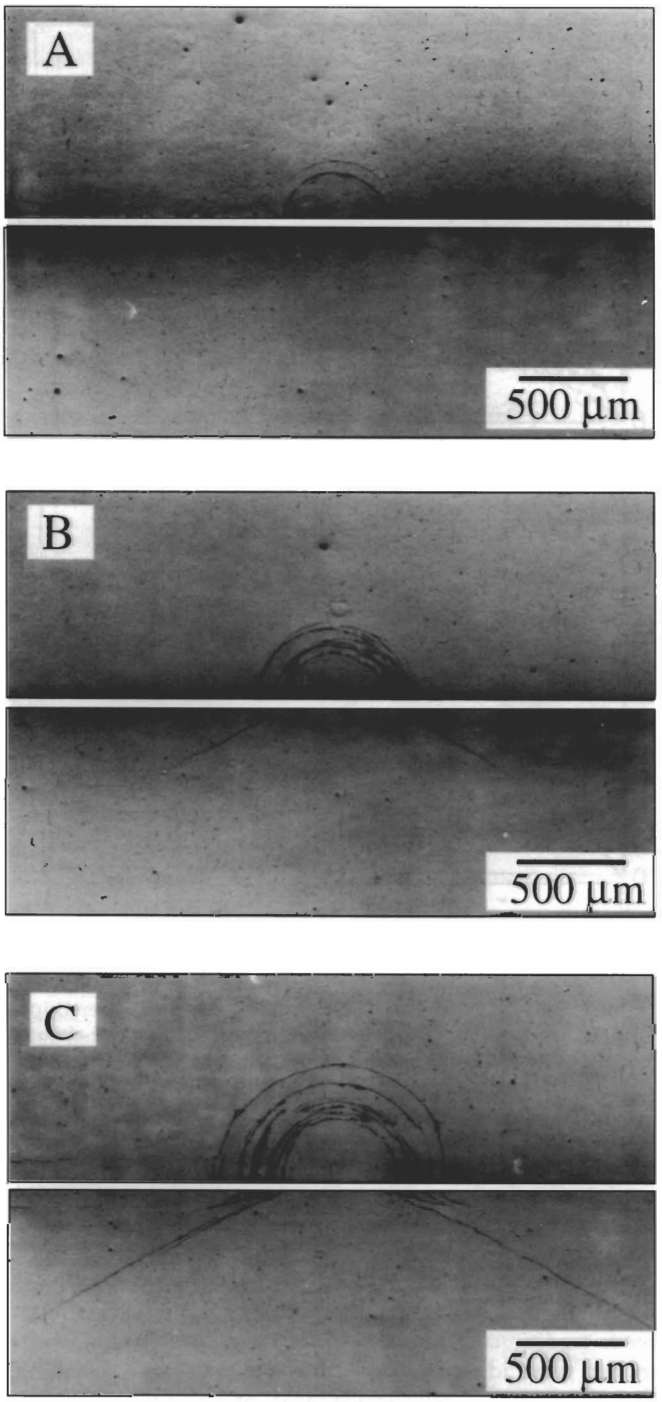

Figure 6. Nomarski optical micrographs, half-surface (upper) and section (lower) views, from bonded-interface specimens of feldspathic porcelain, after indentation with a WC sphere, r = 3.18 mm. Load sequence, (A) P = 250 N, (B) 750 N, (C) 1500 N.

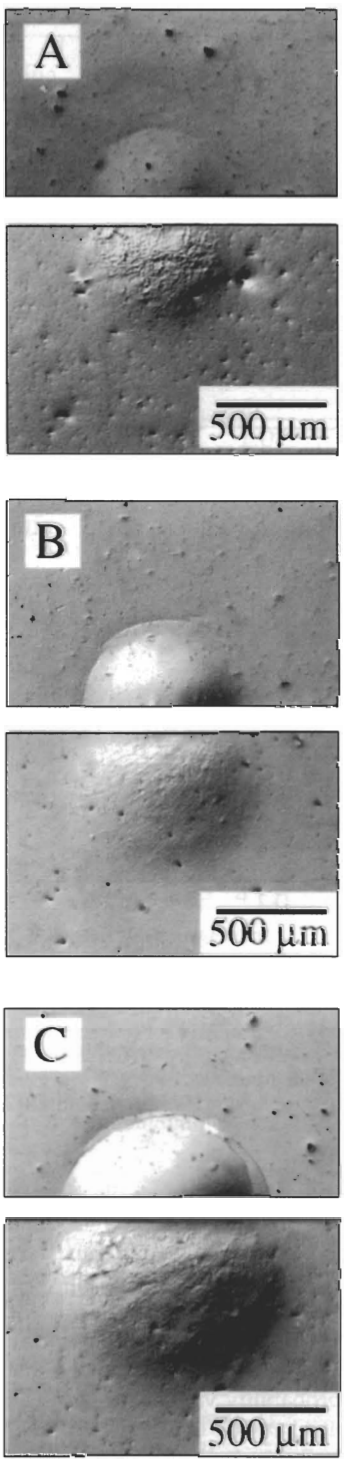

Figure 7. Nomarski optical micrographs, half-surface (upper) and section (lower) views, from bonded-interface specimen of yttria tetragonal zirconia polycrystal (Y-TZP), after indentation with WC sphere, r = 3.18 mm. Load sequence, (A) P = 1000 N, (B) 3000 N, (C) 4750 N.

(Fig. 10), failure occurs from ring cracks in F-MGC and M-MGC, but from subsurface quasi-plastic damage in C-MGC. Strength drops associated with failures from indentation sites are most abrupt for the F-MGC, less so for the M-MGC, and relatively minor for the C-MGC. In the alumina (Fig. 11), failure occurs predominantly from the quasi-plastic damage zone, and only occasionally from cone cracks (at $P > P_C$). As with the C-MGC, the strength losses associated with indentation damage were relatively slight for alumina.

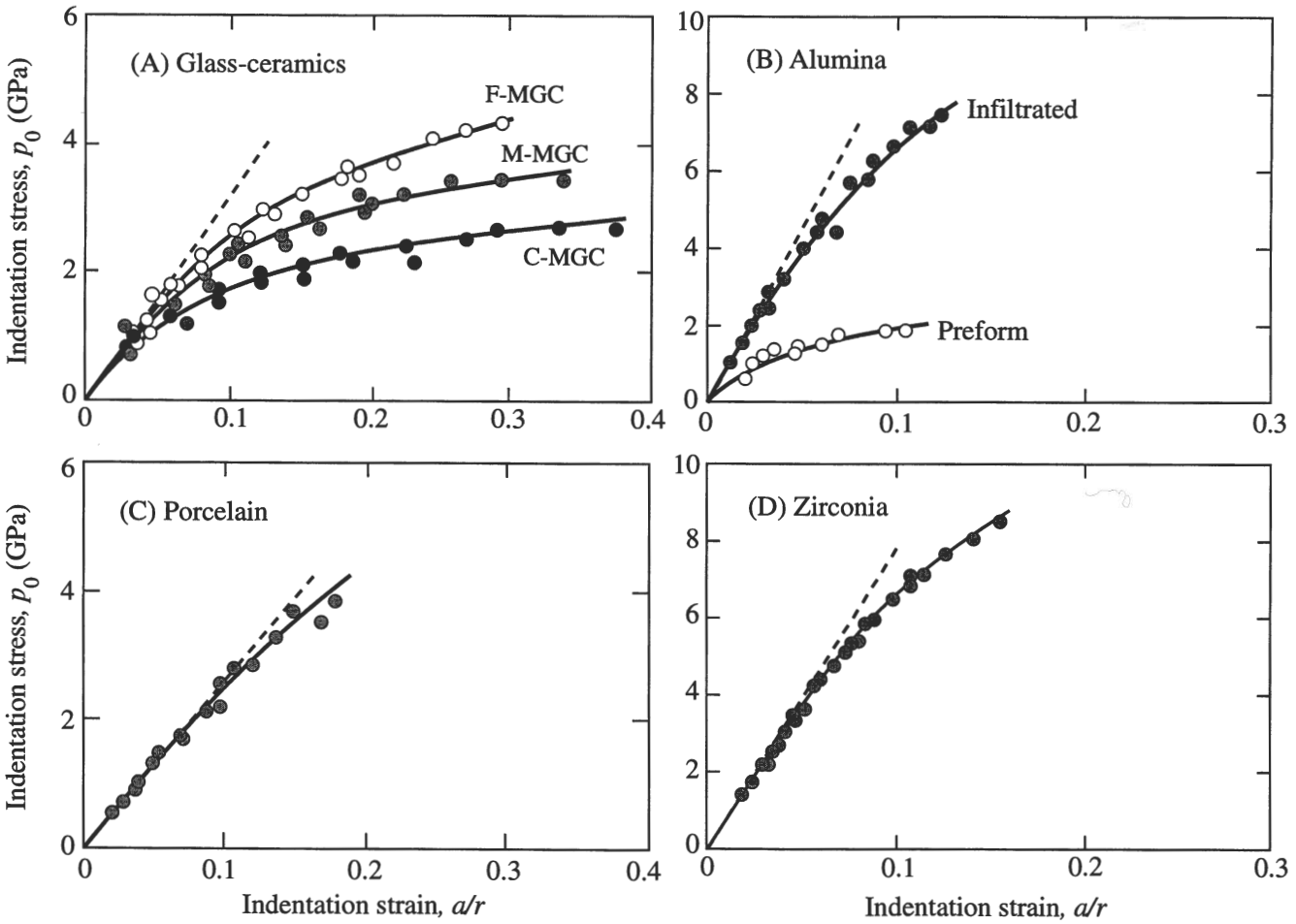

Figure 8. Indentation stress–strain curves: (A) micaceous glass-ceramics, F-MGC, M-MGC, and C-MG [data re-plotted from Fischer-Cripps and Lawn (1996a)]; (B) alumina ceramics, in infiltrated and preform states; (C) feldspathic porcelain; and (D) yttria tetragonal zirconia polycrystal. Test conducted using WC spheres, radii r = 1.98 to 12.7 mm (not distinguished in Fig.). Data points represent individual indentations made on 3 polished specimens of each material, in air, at a crosshead speed 0.2 mm.min^{-1}. Dashed lines are Hertzian limits for ideally elastic contact as linear asymptotic limits at small stresses and strains.

These results indicate that quasi-plastic damage, although not benign, is less deleterious to strength than is fracture.

The significance of the strength differences between representative damage states for the glass-ceramics in Fig. 10 and alumina in Fig. 11 was quantified by ANOVA. Analyses of the strength differences associated with breaks from indentations relative to the as-polished state yielded the following probability values: in F-MGC, $p << 0.001$ ($P >$ 750 N); in M-MGC, $p \approx 0.01$ ($P >$ 750 N); in C-MGC, $p \approx 0.07$ ($P >$ 250 N); and in the infiltrated alumina, $p \approx 0.06$ ($P >$ 500 N). Probability values for strength differences for failures from sandblast damage and indentation sites lie in the range $p << 0.05$, implying that the sandblasting damage was closely equivalent to indentation damage in these materials.

Discussion

In this study, we have presented Hertzian indentation as a protocol for characterizing the mechanical behavior of dental ceramics, using selected generic ceramic systems as case studies. In the materials literature, the Hertzian test has been demonstrated to be an especially simple means of obtaining fundamental insights into potential lifetime-controlling damage modes in ceramics (Lawn *et al.*, 1994a), including modes that may not be immediately detectable by more traditional fracture testing. Two competing damage modes were identified: fracture—ring, or cone, cracking; and deformation—subsurface yield, or quasi-plasticity. We have shown how these two competing modes may be readily identified in dental ceramics using ceramographic techniques. Significantly, the Hertzian test simulates essential features of the loading conditions experienced by restorations in the mouth. The two most accessible measurable Hertzian test quantities, contact (masticatory) force (P) and sphere (cuspal) radius (r), represent important clinical variables. Measurements of indentation stress–strain curves and critical loads for initiation of fracture and deformation enable the damage to be quantitatively characterized. These measurements could be valuable aids to materials ranking and design, and, ultimately, to

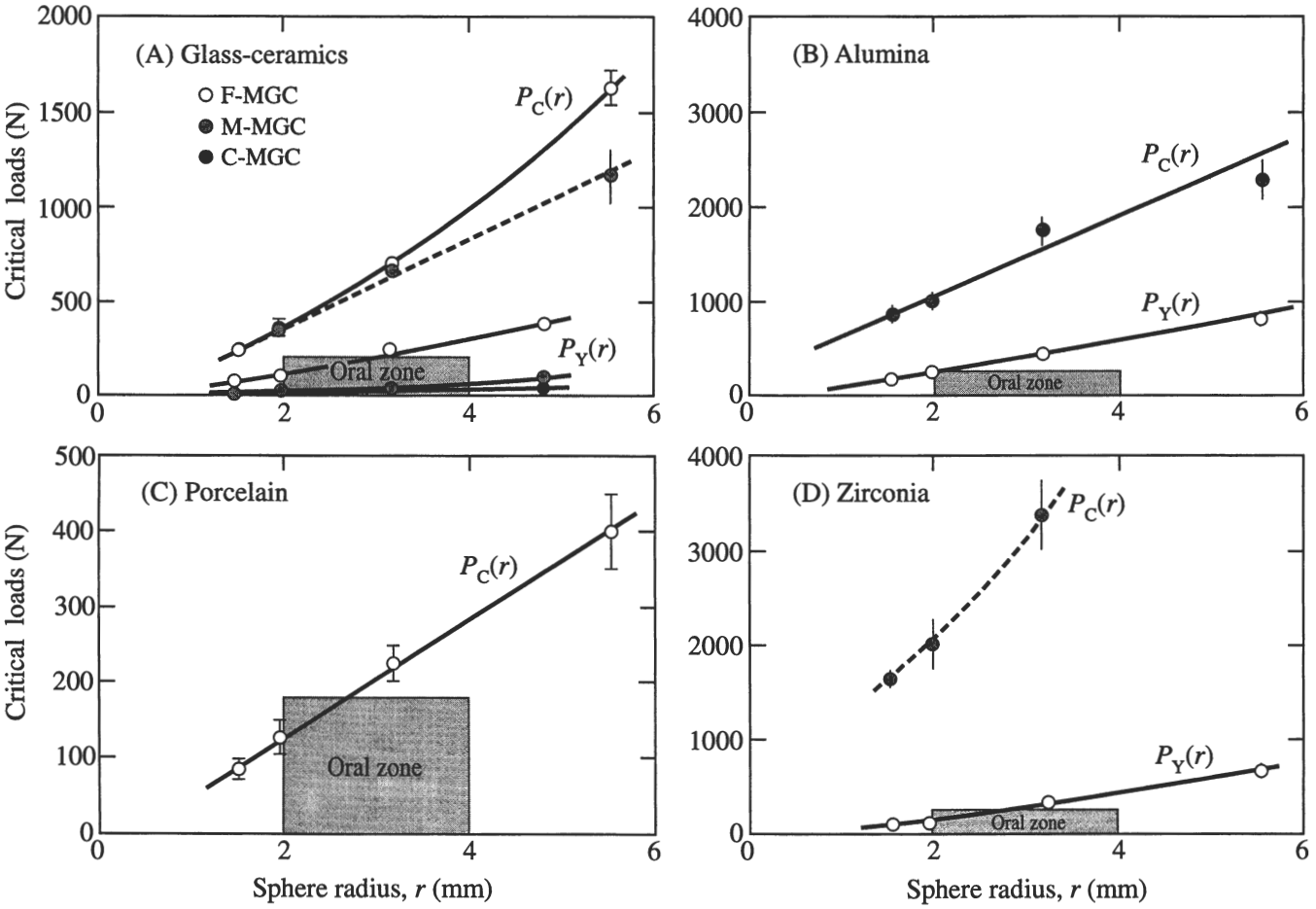

Figure 9. Critical loads for onset of subsurface yield (P_Y) and surface cracking (P_C) as function of WC sphere radius (r), for: (A) micaceous glass-ceramics, F-MGC, M-MGC, and C-MGC; (B) glass-infiltrated alumina; (C) feldspathic porcelain; and (D) yttria tetragonal zirconia polycrystal. Shaded zones indicate "typical" range of oral masticatory conditions. Dashed curves through $P_C(r)$ data indicate incompletely developed, surface-localized ring cracks. Bars with horizontal caps indicate standard deviations, 6 indentations *per* point, acoustic emission crack detection data. Bars without horizontal caps indicate uncertainty range of critical loads determined visually from post-failure Nomarski microscopy of specimen surfaces indented at a series of loads in the vicinity of the thresholds, with a minimum of 6 indentations at each prescribed load. (In some cases, the bars are smaller than the data symbols.)

predictions of clinical lifetimes.

The ceramic systems characterized in the present study cover a broad spectrum of contact responses, from essentially "brittle" (crack-dominated) to essentially "quasi-plastic" (deformation-dominated). These different responses closely reflect the underlying microstructures of the material types. For example, the porcelain exhibits near-classic cone fracture just beyond the fracture threshold (Fig. 6A). At high loads, the expanding contact circle engulfs the trace of the inner surface ring crack and arrests the downward propagating cone, after which multiple, near-concentric outer rings develop (Fig. 6C). Significantly, no accompanying subsurface deformation is evident in Fig. 6, consistent with the relatively slight nonlinearity in the stress–strain curve (Fig. 8C). This porcelain apparently does not possess the weak internal defect structure necessary to initiate local deformation at low contact stresses. [On the other hand, others (White *et al.*, 1995) have measured substantial Hertzian stress–strain nonlinearity in a different dental porcelain (Vita VMK69N), implying the existence of a material with a microstructure weaker than that of the porcelain studied here.] In the micaceous glass-ceramics, a brittle–plastic transition was affected by microstructural coarsening, with ring cracking dominant in F-MGC (Fig. 4A) and quasi-plasticity dominant in C-MGC (Fig. 4C) (Denry *et al.*, 1996; Fischer-Cripps and Lawn, 1996a). This transition is clearly reflected in the shifts in the stress–strain curves for the MGC materials (Fig. 8A). [Indentations on the base glass from which this glass-ceramic system was crystallized reveal an ideal Hertzian cone-crack response, with no detectable quasi-plasticity and no stress–strain nonlinearity (Fischer-Cripps and Lawn, 1996a).] Characteristically, the brittle F-MGC (Fig. 10A) exhibits more abrupt and more severe strength losses than the quasi-plastic C-MGC (Fig. 10C). However, in the C-MGC, failure still occurs from the contact sites, emphasizing that quasi-plasticity damage is not benign. In the harder glass-infiltrated alumina, subsurface quasi-plasticity is the more common source of

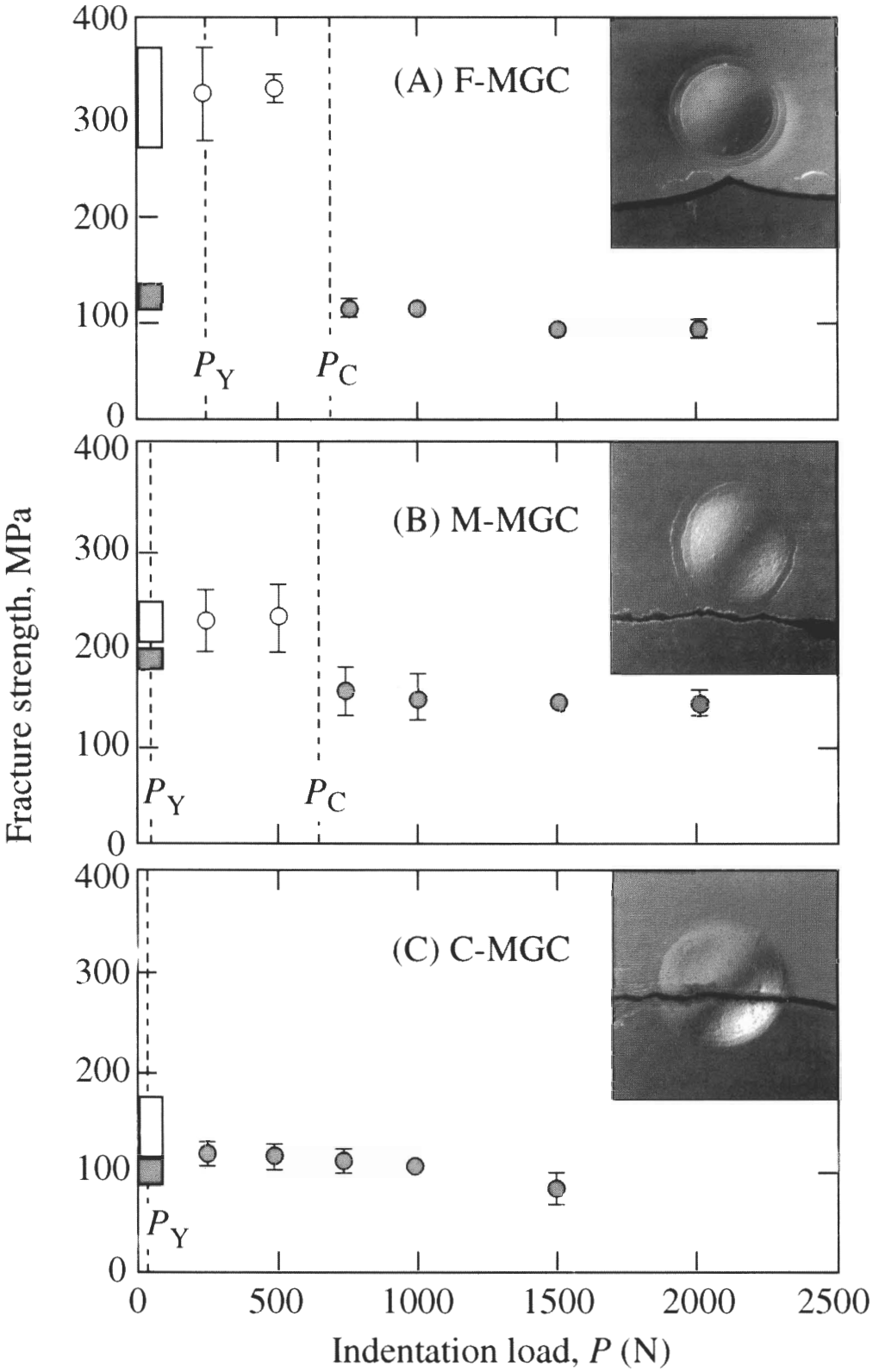

Figure 10. Strength of micaceous glass-ceramic specimens indented with WC sphere, r = 3.18 mm, as function of contact load: (A) F-MGC, (B) M-MGC, (C) C-MGC. Data points are means and standard deviations, 3 to 5 flexure specimens *per* point; closed symbols represent failures from indentation origins, open symbols failures from other origins. Open box at left axis represents strengths of polished, unindented specimens; shaded box represents strengths of sandblasted specimens. Inset micrographs show failure origins at P = 1500 N (tension axis vertical).

ultimate failure in the strength degradation tests (Fig. 11), even when cone-cracking occurs (Fig. 5), and even though the nonlinearity in the stress–strain curve is not strong (Fig. 8B). The retained strengths in this material are much higher than in the glass-ceramics, with relatively slow fall-off at high contact loads, indicative of a damage-tolerant material (Kappert and Knode, 1993). In zirconia, the damage pattern is primarily quasi-plastic (Fig. 7), notwithstanding the fact that its stress–strain curve (Fig. 8D) differs little from that of the alumina. Previous strength degradation studies on a range of zirconia ceramics with Vickers indenters [which invariably introduce more severe fracture damage than their spherical indenter counterparts (Lawn *et al.*, 1975, 1976)] again suggest a high degree of damage tolerance in this material class (Readey *et al.*, 1993).

The $P_Y(r)$ and $P_C(r)$ functions in the critical load diagrams (Fig. 9) are of special clinical interest. Physically, the monotonic increases in these functions reflect a diminished stress concentration with increasing indenter radius at any given contact load (Tabor, 1951; Lawn and Wilshaw, 1975; Lawn, 1993), so that higher values of P are necessary to induce deformation and fracture at larger r. It is the inclusion of the "oral zones" representing masticatory forces and cuspal radii under typical oral conditions (Wheeler, 1958; DeLong and Douglas, 1983; Anusavice, 1989; Phillips, 1991; Craig, 1997) that provides the clinical

relevance. Traversal of the oral zones by the critical load curves implies the likelihood of oral contact damage in the restorative material, suggesting that at small cuspal radii, or in inadvertent contacts with sharp foreign objects during mastication, the critical conditions for damage may well be exceeded. In this sense, the plots in Fig. 9 may be termed "damage maps". Such damage may not always be clearly apparent from casual observations of contact sites. The micaceous glass-ceramics (Fig. 9A) are especially prone to yielding, and the porcelain to cracking (Fig. 9C), suggesting potential susceptibility to failure in oral restorations in both these materials, but from different damage modes. This implied susceptibility is consistent with the high incidence of failures in porcelain and glass-ceramic molar full crown restorations mentioned in the "Introduction" (Hankinson and Cappetta, 1994; Kelsey *et al.*, 1995). In this context, even the alumina (Fig. 9B) and zirconia (Fig. 9D) $P_Y(r)$ data sets intersect the oral zone. In both these materials, $P_Y << P_C$ over the entire range of r shown, confirming quasi-plasticity as the dominant mode of damage. The toughened yttria-stabilized tetragonal zirconia polycrystal is highly crack-resistant, *i.e.*, very high P_C; earlier studies using both Vickers (Readey *et al.*, 1993) and Hertzian indentations (Pajares *et al.*, 1995a,b) suggest that other zirconia compositions could be even more crack-resistant.

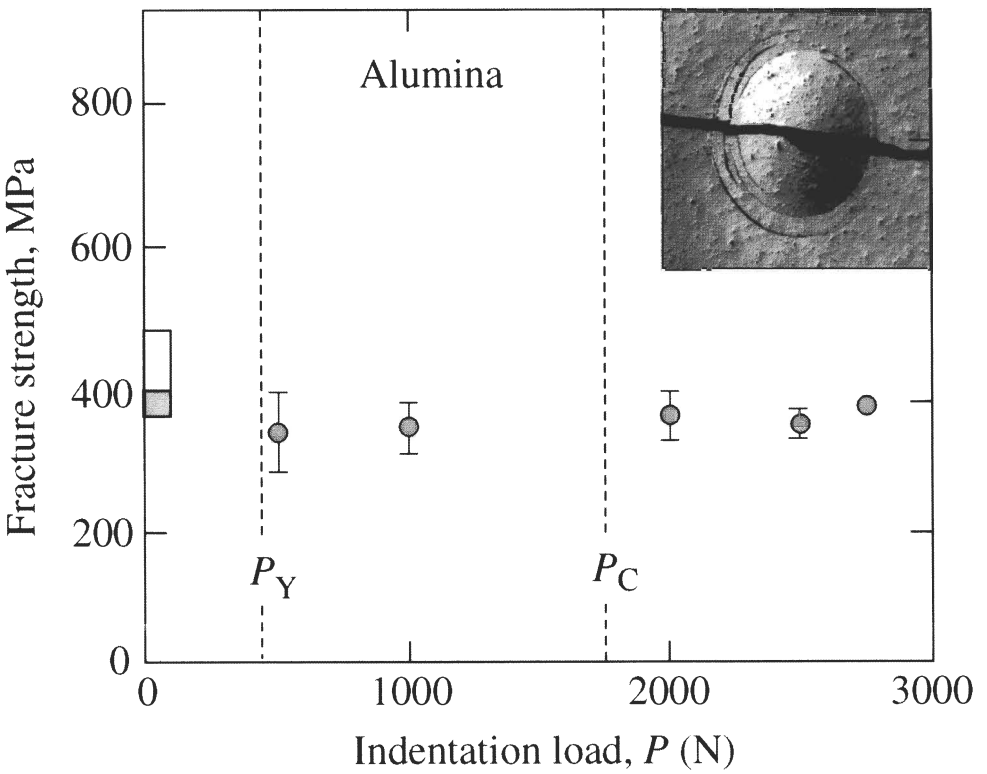

Figure 11. Strength of Hertzian-indented glass-infiltrated alumina specimens with WC sphere, r = 3.18 mm, as function of contact load. Data points are means and standard deviations, 5 flexure specimens *per* point; closed symbols represent failures from indentation origins, open symbols failures from other origins. Open box at left axis represents strengths of polished, unindented specimens; shaded box represents strengths of sandblasted specimens. Inset micrograph indicates subsurface damage failure origin at P = 2750 N (tension axis vertical).

There is the further issue of how damage evolves as the load increases above the damage thresholds. Both cracks (porcelain, Fig. 6) and quasi-plastic damage (zirconia, Fig. 7) grow steadily with increasing contact load. In less-brittle materials, it is conceivable that the onset of deformation could impart some clinical benefit, by broadening subsequent occlusal contacts and thereby reducing stress intensities. In restorations, failure will occur when the characteristic dimension of the damage approaches some significant fraction of the restoration thickness, or when non-contact (*e.g.*, flexure) stresses exceed the strength level for the material.

We would caution against the argument that Hertzian testing with hard spheres represents uncommonly intense stress states, and is therefore likely to overestimate the susceptibility of dental ceramics to damage and ensuing failure. It is true that the WC spheres used here have much higher modulus and hardness than tooth enamel. However, even soft indenters can cause substantial damage in harder materials, because indentation stresses continue to rise well beyond the initial yield stress with monotonically increasing load, saturating in the high strain region at approximately the hardness value (as measured by conventional Vickers indenter) (Tabor, 1951). Note that the hardness of enamel, ≈ 3 to 4 GPa (Craig and Peyton, 1958), lies within the quasi-plasticity region of the stress–strain curves for the softer materials in Fig. 8. Moreover, the data presented in this work represent single-cycle contacts, in laboratory atmospheres. Actual masticatory conditions can be considerably more severe. Quite apart from inadvertent biting on sharp foreign objects, restorations are subject to repeated loading over long periods, with superposed tangential motion, in chemically active aqueous environments, all of which could greatly exacerbate damage build-up (DeLong and Douglas, 1983; Kappert and Knode, 1993). Hertzian testing can be readily extended to such conditions, *e.g.*, by repeating the number of contacts (Guiberteau *et al.*, 1993; Cai *et al.*, 1994b; Padture and Lawn, 1995a; Pajares *et al.*, 1995b; White *et al.*, 1995), by superimposing a sliding force (Lawn, 1967; Lawn *et al.*, 1984), and by immersing the specimens in appropriate fluids (Langitan and Lawn, 1970;

Guiberteau et al., 1993). Previous "contact fatigue" tests of this kind on glasses and ceramics under such deleterious conditions reveal greatly accelerated accumulation of damage. Again, the sharp increase in clinical failure rates of some molar ceramic posterior crowns after some years in service (Hankinson and Cappetta, 1994; Kelsey *et al.*, 1995) highlights the importance of fatigue in limiting the longevity of restorations.

The Hertzian test also provides insight into the types of damage and strength degradation likely to occur from common dental laboratory procedures, such as removal of investments from crowns by sandblasting. The glass-ceramic data in Fig. 10 reveal significant drops in strength from sandblasting damage (approximately equivalent to high-load Hertzian contacts). Note that the retained strengths after damage are higher for the intermediate M-MGC than for either F-MGC or C-MGC, implying the need for some kind of compromise in the microstructural design for optimal damage tolerance.

There are several clinical factors, apart from aesthetics and cost, that need to be considered when conclusions from Hertzian testing are drawn. Paramount among these are:

(i) Machinability and wear. Just as increasing microstructural heterogeneity reduces the tendency of ceramics to large-scale fracture, it simultaneously increases the susceptibility to material disintegration at the microstructural level (Padture and Lawn, 1995b). This susceptibility leads to easier machinability in materials that ordinarily might be regarded as brittle, especially in micaceous glass-ceramics (Chyung *et al.*, 1972, 1974) and alumina preforms (Wolf, 1995; Wolf *et al.*, 1996). At the same time, it renders the ceramics more prone to material removal by fatigue (Guiberteau *et al.*, 1993; Cai *et al.*, 1994b; Padture and Lawn, 1995a) and wear (Xu *et al.*, 1995; Nagarajan and Jahanmir, 1996; Xu *et al.*, 1996). Optimizing the microstructure of any given class of ceramic for machinability, damage tolerance, wear resistance, and fatigue resistance may require considerable compromise.

(ii) Core–veneer design. Aesthetically and mechanically, porcelain and glass-ceramics best match the properties of tooth enamel and are most appropriate as cosmetic restoratives. Alumina and zirconia are much more damage-tolerant, but without the aesthetic appeal, and so are more suitable as core materials, subsequently to be veneered (usually with porcelain). Ultimately, it is essential that any given ceramic be considered in the proper context of its likely clinical structure, *i.e.*, in possible combination with other materials with potentially widely different properties. Failures in multilayer ceramic restorations have been noted clinically and have been modeled by finite element analysis (Kelly *et al.*, 1995). In this context, the Hertzian test is currently being extended to the investigation of layered material systems (An *et al.*, 1996; Wuttiphan *et al.*, 1996) that simulate the structures of dental restorations.

The Hertzian test, despite its simplicity, requires care in application, particularly in the use of measurement techniques and the interpretation of ceramographic observations. The bonded-interface technique described in the preceding sections is a particular case in point. Previous bonded-interface tests on dense, high-purity aluminas (Guiberteau *et al.*, 1994) reveal essentially the same subsurface damage zones as those observed in sections polished *after* indentation (translucency enabling the damage to be observed by light-scattering in those materials) (Guiberteau *et al.*, 1993). Nevertheless, artifacts can arise if the adhesive used to bond the opposing half-blocks is not thin enough (typically < 5 μm) (Guiberteau *et al.*, 1994). It is for this reason that a small clamping pressure is often applied during contact testing, to prevent premature interfacial separation. Even with the greatest care in preparation, the bonded-interface specimen cannot be expected to reproduce faithfully every detail of the damage geometry in bulk specimens. For example, a ring crack initiated in one half-block cannot traverse the soft cyano-acrylate interface, so that somewhat different crack populations can exist in opposite half-blocks. Comparisons with polished sections nevertheless indicate that the crack geometries are qualitatively representative of those in bulk specimens, even if absolute values of critical contact variables (such as P_C and P_Y) may differ as much as 10 to 20% (Lee *et al.*, 1997). In some microstructures, *e.g.*, fine-grain glass-ceramics (Fig. 4A), not even ultra-sensitive Nomarski interference contrast is capable of revealing quasi-plastic damage clearly, despite evidence for the existence of this damage from the corresponding stress–strain and critical load (P_Y) measurements. In such instances, even more sensitive methods of damage detection—such as two-beam interference microscopy (Pajares *et al.*, 1995b), thermal wave imaging (Wei and Lawn, 1996), and surface profilometry (or even atomic force microscopy)—have been proven useful.

Under most conventional ceramics testing conditions, failure occurs most often by classic crack growth, driven by tensile stresses. In contact fields, however, quasi-plasticity processes, driven by shear stresses, can dominate the failure mechanics. Development of superior materials for the clinician will depend on a fundamental understanding of both the deformation and fracture modes, especially in the context of microstructure. Ultimately, a proper understanding of microstructure–properties relationships will require appropriate modeling of the damage processes. Modeling of contact quasi-plasticity at the macroscopic level by finite element modeling (Fischer-Cripps and Lawn, 1996a) and at the microscopic level in terms of shear fault micromechanics (Lawn *et al.*, 1994b; Padture and Lawn, 1995b; Fischer-Cripps and Lawn, 1996b; Lawn and Marshall, 1998) has begun. Together with such modeling, and along with relevant clinical data, the Hertzian contact test presents itself as a powerful methodology for the development of the next generation of dental ceramics.

Acknowledgments

The authors acknowledge the generous supply of materials from Ken Chyung at Corning Inc., Helga Hornberger at Vita Zahnfabrik, and Jack Sibold at Coors Ceramics. They also thank H.H.K. Xu, J.R. Kelly, A.C. Fischer-Cripps, and D.B. Marshall for helpful discussions on various aspects of this work. This work was partially funded under NIDR Grant PO1 DE10976.

References

An L, Chan HM, Padture NP, Lawn BR (1996). Damage-resistant alumina-based layer composites. *J Mater Res* 11:204-210.

Anusavice KJ (1989). Criteria for selection of restorative materials: properties *vs* technique sensitivity. In: Quality evaluations of dental restorations. Anusavice KJ, editor. Chicago: Quintessence, pp. 15-56.

Cai H, Kalceff MAS, Hooks BM, Lawn BR, Chyung K (1994a). Cyclic fatigue of a mica-containing glass–ceramic at Hertzian contacts. *J Mater Res* 9:2654-2661.

Cai H, Kalceff MAS, Lawn BR (1994b). Deformation and fracture of mica-containing glass–ceramics in Hertzian contacts. *J Mater Res* 9:762-770.

Chyung CK, Beall GH, Grossman DG (1972). Microstructures & mechanical properties of mica glass-ceramics. In: Electron microscopy and structure of materials. Thomas G, Fulrath RM, Fisher RM, editors. Berkeley, CA: University of California Press, pp. 1167-1194.

Chyung CK, Beall GH, Grossman DG (1974). Fluorophlogopite mica glass-ceramics. In: Proceedings of 10th International Glass Congress, No. 14, Kunugi M, Tashiro M, Saga N, editors. Tokyo, Japan: The Ceramic Society of Japan, Kyoto, pp. 33–40.

Craig RG (1997). Mechanical properties. In: Restorative dental materials. Craig RG, editor. St. Louis: Mosby, Chapter 4.

Craig RG, Peyton FA (1958). The microhardness of enamel and dentin. *J Dent Res* 37:661-668.

Dauskardt RH (1993). A frictional wear mechanism for fatigue-crack growth in grain bridging ceramics. *Acta Metall Mater* 41:2765-2781.

Dauskardt RH, Marshall DB, Ritchie RO (1990). Cyclic fatigue–crack propagation in magnesia-partially-stabilized zirconia ceramics. *J Am Ceram Soc* 73:893-903.

Davies RM (1949). Determination of static and dynamic yield stresses using a steel ball. *Proc R Soc Lond* 197(A):416-432.

DeLong R, Douglas WH (1983). Development of an artificial oral environment for the testing of dental restoratives: bi-axial force and movement control. *J Dent Res* 62:32-36.

Denry IL, Rosenstiel SF (1995). Hertzian indentation response of Dicor machinable glass-ceramics (abstract). *J Dent Res* 74:522.

Denry IL, Holloway JA, Gourlaouen V, Johnston WM, Rosenstiel SF (1996). Hertzian indentation response of mica-containing dental glass-ceramics (abstract). *J Dent Res* 75:858.

Fischer-Cripps AC, Lawn BR (1996a). Indentation stress–strain curves for "quasi-ductile" ceramics. *Acta Metall* 44:519-527.

Fischer-Cripps AC, Lawn BR (1996b). Stress analysis of contact deformation in quasi-plastic ceramics. *J Am Ceram Soc* 79:2609-2618.

Frank FC, Lawn BR (1967). On the theory of Hertzian fracture. *Proc R Soc Lond* 299(A):291-306.

Giordano RA (1996). Dental ceramic restorative systems. *Compend Contin Educ Dent* 17:779-782, 784-786 *passim*, 794.

Grossman DG (1991). Structure and physical properties of Dicor/MGC glass-ceramic. In: Proceedings of the international symposium on computer restorations. Mörmann WH, editor. Chicago, IL: Quintessence Publishing Co., pp. 103-115.

Guiberteau F, Padture NP, Cai H, Lawn BR (1993). Indentation fatigue: a simple cyclic Hertzian test for measuring damage accumulation in polycrystalline ceramics. *Phil Mag* 68(A):1003-1016.

Guiberteau F, Padture NP, Lawn BR (1994). Effect of grain size on Hertzian contact in alumina. *J Am Ceram Soc* 77:1825-1831.

Hankinson JA, Cappetta EG (1994). Five years clinical experience with a leucite-reinforced porcelain crown system. *Int J Perio Rest Dent* 14:138-153.

Harvey CK, Kelly JR (1996). Contact damage as a failure mode during *in vitro* testing. *J Prosthodont* 5:95-100.

Hertz H (1896). Hertz's miscellaneous papers. London: Macmillan, Chapters 5, 6.

Kappert H, Knode H (1993). InCeram: testing a new ceramic material. *Quintessence Dent Technol* 16:87-97.

Kelly JR, Giordano R, Pober R, Cima MJ (1990). Fracture surface analysis of dental ceramics: clinically failed restorations. *Int J Prosthodont* 3:430-440.

Kelly JR, Tesk JA, Sorensen JA (1995). Failure of all-ceramic fixed partial dentures *in vitro* and *in vivo*: analysis and modeling. *J Dent Res* 74:1253-1258.

Kelsey WP, Cavel T, Blankenau RJ, Barkmeier WW, Wilwerding TM, Latta MA (1995). 4-year clinical study of castable ceramic crowns. *Am J Dent* 8:259-262.

Langitan FB, Lawn BR (1970). Effect of a reactive environment on the Hertzian strength of brittle solids. *J Appl Phys* 41:3357-3365.

Lathabai S, Lawn BR (1989). Fatigue limits in noncyclic loading of ceramics with crack-resistance curves. *J Mater Sci* 24:4298-4306.

Lathabai S, Mai Y-W, Lawn BR (1989). Cyclic fatigue behavior of an alumina ceramic with crack-resistance curves. *J Am Ceram Soc* 72:1760-1763.

Lathabai S, Rödel J, Lawn BR (1991). Cyclic fatigue from frictional degradation at bridging grains in alumina. *J Am Ceram Soc* 74:1340-1348.

Lawn BR (1967). Partial cone crack formation in a brittle material loaded with a sliding indenter. *Proc R Soc Lond* 299(A):307-316.

Lawn BR (1993). Fracture of brittle solids. Cambridge: Cambridge University Press.

Lawn BR, Marshall DB (1998). Nonlinear stress–strain curves for solids containing closed cracks with friction. *J Mechan Phys Solids* 46:85-113.

Lawn BR, Wilshaw TR (1975). Indentation fracture: principles and applications. *J Mater Sci* 10:1049-1081.

Lawn BR, Wiederhorn SM, Johnson H (1975). Strength degradation of brittle surfaces: blunt indenters. *J Am Ceram Soc* 58:428-432.

Lawn BR, Fuller ER, Wiederhorn SM (1976). Strength degradation of brittle surfaces: sharp indenters. *J Am Ceram Soc* 59:193-197.

Lawn BR, Wiederhorn SM, Roberts DE (1984). Effect of sliding friction forces on the strength of brittle materials. *J Mater Sci* 19:2561-2569.

Lawn BR, Padture NP, Cai HD, Guiberteau F (1994a). Making ceramics "ductile". *Science* 263:1114-1116.

Lawn BR, Padture NP, Guiberteau F, Cai H (1994b). A model for microcrack initiation and propagation beneath Hertzian

contacts in polycrystalline ceramics. *Acta Metall* 42:1683-1693.

Lee SK, Wuttiphan S, Lawn BR (1997). Role of microstructure in Hertzian contact damage in silicon nitride: I. Mechanical characterization. *J Am Ceram Soc* 80:2367-2381.

Marshall DB, Lawn BR (1980). Flaw characteristics in dynamic fatigue: the influence of residual contact stresses. *J Am Ceram Soc* 63:532-536.

Marshall DB, Lawn BR, Chantikul P (1979). Residual stress effects in sharp-contact cracking: ii. Strength degradation. *J Mater Sci* 14:2225-2235.

Mulhearn TO (1959). The deformation of metals by Vickers-type pyramidal indenters. *J Mechan Phys Solids* 7:85-96.

Nagarajan VS, Jahanmir S (1996). Relationship between microstructure and wear of mica-containing glass-ceramics. *Wear* 200:176-185.

Padture NP, Lawn BR (1994). Toughness properties of a silicon carbide with an *in-situ*-induced heterogeneous grain structure. *J Am Ceram Soc* 77:2518-2522.

Padture NP, Lawn BR (1995a). Contact fatigue of a silicon carbide with a heterogeneous grain structure. *J Am Ceram Soc* 78:1431-1438.

Padture NP, Lawn BR (1995b). Fatigue in ceramics with interconnecting weak interfaces: a study using cyclic Hertzian contacts. *Acta Metall* 43:1609-1617.

Pajares A, Guiberteau F, Lawn BR (1995a). Hertzian contact damage in magnesia-partially-stabilized zirconia. *J Am Ceram Soc* 78:1083-1086.

Pajares A, Wei L, Lawn BR (1995b). Damage accumulation and cyclic fatigue in Mg-PSZ at Hertzian contacts. *J Mater Res* 10:2613-2625.

Phillips R (1991). Skinner's science of dental materials. Philadelphia: W.B. Saunders.

Readey MJ, McCallen CL, McNamara P, Lawn BR (1993). Correlations between flaw tolerance and reliability in zirconia. *J Mater Sci* 28:6748-6752.

Rekow D (1993). Hi-tech innovations—and limitations—for restorative dentistry. In: Dental clinics of North America. Halpern B, editor. Philadelphia: W.B. Saunders, pp. 513-524.

Rekow ED (1992). A review of the developments in dental CAD/CAM systems. *Curr Sci: Curr Opin Prosthodont* 2:25-33.

Ritchie RO (1988). Mechanisms of fatigue crack propagation in metals, ceramics, composites: role of crack-tip shielding. *Mater Sci Eng* 103(A):15-28.

Roesler FC (1956). Brittle fractures near equilibrium. *Proc Phys Soc Lond* 69(B):981-992.

Seghi RR, Sorensen JA (1995). Relative flexural strength of six new ceramic materials. *Int J Prosthodont* 8:239-246.

Suresh S (1991). Fatigue of materials. Cambridge: Cambridge University Press.

Swain MV, Hagan JT (1976). Indentation plasticity and the ensuing fracture of glass. *J Phys D: Appl Phys* 9:2201-2214.

Swain MV, Lawn BR (1969). A study of dislocation arrays at spherical indentations in LiF as a function of indentation stress and strain. *Physica Status Solidi* 35:909-923.

Tabor D (1951). Hardness of metals. Oxford: Clarendon.

Thompson JY, Anusavice KJ, Naman A, Morris HF (1994). Fracture surface characterization of clinically failed all-ceramic crowns. *J Dent Res* 73:1824-1832.

Timoshenko S, Goodier JN (1951). Theory of elasticity. New York: McGraw-Hill.

Wei LH, Lawn BR (1996). Thermal wave analysis of contact damage in ceramics: case study on alumina. *J Mater Res* 11:939-947.

Wheeler RC (1958). A textbook of dental anatomy and physiology. Philadelphia, PA: W.B. Saunders, pp. 354-358.

White SN, Zhao XY, Zhaokun Y, Li ZC (1995). Cyclic mechanical fatigue of a feldspathic dental porcelain. *Int J Prosthodont* 8:413-420.

Wilshaw TR (1971). The Hertzian fracture test. *J Phys D: Appl Phys* 4:1567-1581.

Wolf WD (1995). Strength and fracture toughness of alumina-glass dental composites prepared by melt-infiltration (PhD dissertation). Minneapolis: University of Minnesota.

Wolf WD, Vaidya KJ, Francis LF (1996). Mechanical properties and failure analysis of alumina-glass dental composites. *J Am Ceram Soc* 79:1769-1776.

Wuttiphan S, Lawn BR, Padture NP (1996). Crack suppression in strongly-bonded homogeneous/heterogeneous laminates: a study on glass/glass-ceramic bilayers. *J Am Ceram Soc* 79:634-640.

Xu HHK, Padture NP, Jahanmir S (1995). Effect of microstructure on material removal mechanisms and damage tolerance in abrasive machining of silicon carbide. *J Am Ceram Soc* 78:2443-2448.

Xu HHK, Smith DT, Jahanmir S (1996). Influence of microstructure on indentation and machining of dental glass-ceramics. *J Mater Res* 11:2325-2337.